Tracking the electron recapture in dissociative frustrated double ionization of D_2

Wenbin Zhang,[1] Hui Li,[1] Xiaochun Gong,[1] Peifen Lu,[1] Qiying Song,[1] Qinying Ji,[1] Kang Lin,[1] Junyang Ma,[1] Hanxiao Li,[1] Fenghao Sun,[1] Junjie Qiang,[1] Heping Zeng,[1] and Jian Wu[1,2,*]

[1]*State Key Laboratory of Precision Spectroscopy, East China Normal University, Shanghai 200062, China*

[2]*Collaborative Innovation Center of Extreme Optics, Shanxi University, Taiyuan, Shanxi 030006, China*

(Received 9 April 2018; published 23 July 2018)

By measuring the ejected neutral and ionic fragments as well as the freed electron in coincidence, we track the laser induced dissociative frustrated double ionization (FDI) of D_2, in which process one of the two tunneled electrons is eventually recaptured by the outgoing nuclei of the breaking molecule after the conclusion of the femtosecond laser fields. The dynamics are investigated in a pump-probe scheme by using an elliptically and linearly polarized few-cycle laser pulses with tunable time delay. The distinct momentum distributions of the escaped electrons governed by the light polarizations allow us to identify from which laser fields, i.e., the pump or the probe fields, the electron is released and thus deduce the origin of the recaptured one. Our results show that the electron released in the second ionization step after the stretching of molecular bond is favored to be recaptured in the dissociative FDI of molecules.

DOI: 10.1103/PhysRevA.98.013419

I. INTRODUCTION

When molecules are exposed to strong laser fields, the excitation of electron from bound states to the continua gives rise to a multitude of intriguing phenomena, such as the bond-softening and hardening [1–4], the electron-nuclear sharing of the absorbed photon energy [5–9], the nonsequential double ionization [10–12], the laser-induced Coulomb explosion [13–15], and the charge-resonance enhanced ionization (CREI) [16–19]. After the conclusion of the laser pulse, besides escaping to the continuum, a substantial fraction of the detached electrons that does not gain sufficient drift energy from the laser field would be recaptured by the Coulomb potential of the positively charged ionic core and eventually be trapped into the high-lying Rydberg orbitals, which is intuitively dubbed as the "Coulomb recapture effect" [20] or "frustrated tunneling ionization (FTI)" [21].

The strong-field induced FTI has been observed for both atoms [22–24] and molecules [25–33]. For the Coulomb-explored double ionization of molecules, there is a certain probability that one of the two tunneled electrons escapes and the other one is recaptured to one of the outgoing ionic fragments, leading to the dissociative frustrated double ionization (FDI) [34]. Depending on whether the recaptured electron is released in the first or the second ionization step, two routes were theoretically predicted for the dissociative FDI of H_2 [27]. However, due to the coexistence of the first and second ionization steps within a multicycle femtosecond laser pulse, the question of which ionization step governs the dissociative FDI of molecules stands yet to date experimentally unexplored.

In this paper, we experimentally tracked the electron recapture dynamics for the dissociative FDI of D_2, i.e., $D_2 + n\hbar\omega \rightarrow {D_2}^+ + e_1 + m\hbar\omega \rightarrow D^+ + D^+ + e_2 \rightarrow D^+ + D^* + e$, denoted as the ($D^+$, D^*) channel, by using elliptically and linearly polarized few-cycle laser pulses in a pump-probe scheme. It allows us to disentangle the first and second ionization steps by sequentially removing two electrons from D_2 by the few-cycle pump and probe pulses. We note that no (D^+, D^*) channel is observed in a single few-cycle pulse which is too short to drive the sequential process characterized by the stretching of the molecular ion created in the first ionization step. The stepwise dynamics of the dissociative FDI of D_2 can be mapped by tracing the motion of the dissociating nuclear wave packet (NWP) on the potential-energy curves of ${D_2}^+$ as a function of the time delay between the pump and probe pulses. The measured final momentum distributions of the escaping electrons governed by the laser polarizations allow us to identify from which laser pulse it is released and thus deduce the origin of the recaptured one. The electron tunneled in the second ionization step is found to dominate the formation of neutral Rydberg atoms in the dissociative FDI of molecules.

II. EXPERIMENTAL METHOD

In the experiment, we perform the measurements in an ultrahigh-vacuum reaction microscope of cold target recoil ion momentum spectroscopy (COLTRIMS) [35,36]. As schematically illustrated in Fig. 1(a), the D^+ ion created through photoionization will be accelerated by the static electric field of the spectrometer ($E_s \sim 12.7\,\mathrm{V/cm}$) towards the ion detector and detected regardless of its initial ejection direction. The produced excited neutral D^* can only be detected if it flies towards the ion detector and impinges on the microchannel plate (MCP) detector with an internal potential energy beyond the work function of the MCP (a few eV) [37]. Meanwhile, the freed electron accelerated by E_s of the spectrometer and guided by a weak magnetic field ($B \sim 11$ G) will be detected by the electron detector. The three-dimensional momenta of

*jwu@phy.ecnu.edu.cn

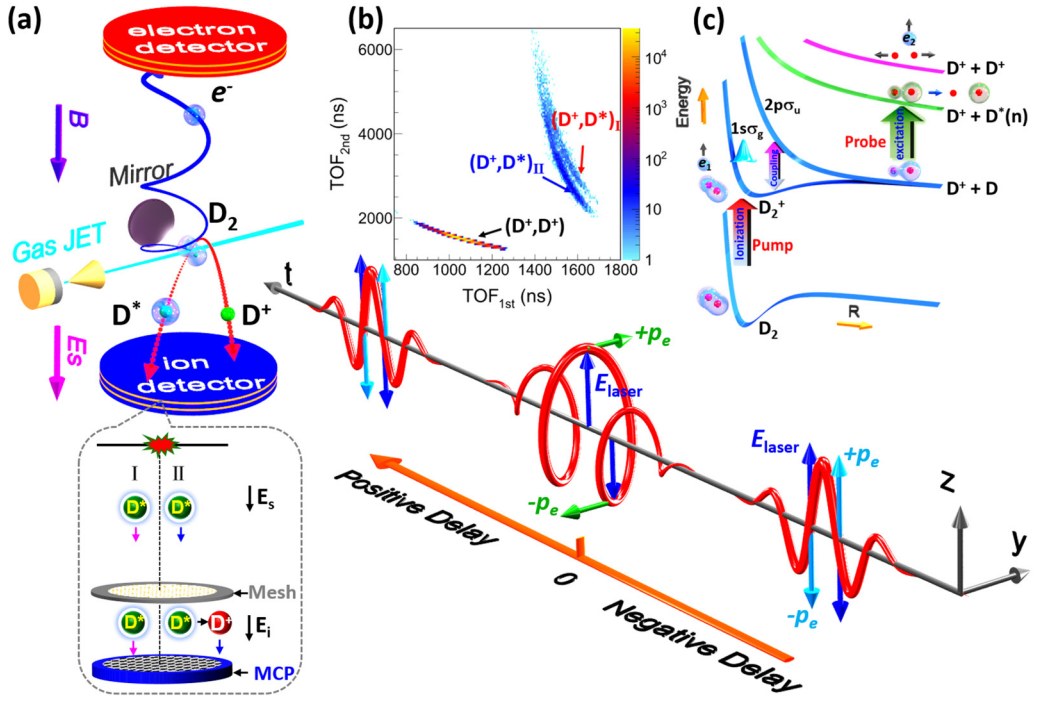

FIG. 1. (a) Schematic view of the experimental setup. The inset on the bottom left shows the illustration of the spectrometer configuration of the ion side of the COLTRIMS apparatus. (b) Measured PIPICO spectrum of the (D^+, D^+) and (D^+, D^*) channels produced from the strong-field dissociative double ionization of D_2. (c) Schematic illustration of the stepwise dynamics of the dissociative FDI of D_2 driven by the few-cycle pump and probe pulses.

the detected particles were reconstructed from the measured times of flight (TOFs) and positions of the impacts during the offline analysis.

An elliptically and a linearly polarized few-cycle laser pulses in a pump-probe arrangement is employed to pump and probe the dissociative FDI process. To generate the few-cycle pulses, linearly polarized near-infrared femtosecond laser pulses (25 fs, 790 nm, 10 kHz, polarized along the y axis) delivered from a multipass Ti:sapphire amplifier were spectrally broadened in an argon-filled hollow-core fiber and afterwards temporally compressed using pairs of chirped mirrors. The laser beam was then fed through a Mach-Zehnder interferometer to produce the pump and probe few-cycle pulses in two arms with linear and elliptical polarizations, respectively. The polarization of the linear arm was rotated to be along the TOF direction of the spectrometer (the z axis) by using a half-wave plate (HWP). For the other arm, the laser polarization was adjusted to be elliptically polarized in the y-z plane with the major axes along the z axis by utilizing a quarter-wave plate (QWP) in combination with a HWP. The fast axis of the QWP was fixed to be along the z axis and the ellipticity of the ellipse was adjusted to be ~0.72 by varying the orientation of the fast axis of the HWP placed in front of the QWP. The time delay between the pump and probe pulses was finely controlled by using a motorized delay stage. The pulses were afterwards tightly focused onto a supersonic gas jet of D_2 by a concave silver mirror ($f = 7.5$ cm) inside the COLTRIMS. By tracing the time-delay-dependent yield of the singly ionized molecules, we estimate the temporal duration of the few-cycle pulse to be ~7 fs (full width at half maximum). The intensities of the linearly and elliptically polarized few-cycle pulses in the interaction region were estimated to be 6.8×10^{14} W/cm^2 and 1.0×10^{15} W/cm^2, respectively.

III. RESULTS AND DISSUSSIONS

To identify the (D^+, D^*) nuclear fragment pair produced from the dissociative FDI of D_2, the photoion-photoion coincidence (PIPICO) spectrum of the nuclear fragments is employed. As compared to the ionic D^+, the neutral D^* flies to the ion detector with the mere recoil momentum gained from the dissociation in defect of the acceleration by the static electric field E_s of the spectrometer and exhibits a much larger TOF than that of the D^+. As shown in Fig. 1(b), the (D^+, D^*) pair is clearly distinguished from the Coulomb-exploded double ionization channel of (D^+, D^+), i.e., $D_2 + m\hbar\omega \rightarrow D^+ + D^+ + 2e$ in the PIPICO spectrum. For the excited neutral atom, the solid angle of detection is determined by the geometry of the spectrometer which is about 0.9π sr in our experiment [34]. The momentum conservation of the measured ionic D^+, the neutral Rydberg atom D^* and the freed electron of the three-body breakup channel of (D^+, D^*) allows us to unambiguously identify the dissociative FDI channel. To suppress the false coincidence, a momentum conservation gate of $|p_{z,D^+} + p_{z,D^*} + p_{z,e(\text{freed})}| < 0.5$ a.u. along the TOF direction of the spectrometer is applied. The dual PIPICO lines of the (D^+, D^*) pair, indicated as (D^+, D^*)$_I$ and (D^+, D^*)$_{II}$ in Fig. 1(b), are related to the field ionization of the laser-created Rydberg atoms [38–43]. As illustrated in the inset of Fig. 1(a), the laser-created D^* that survived from E_s (~12.7 V/cm) of the spectrometer can be directly detected by the MCP as D^*, forming the (D^+, D^*)$_I$, or be indirectly detected as D^+

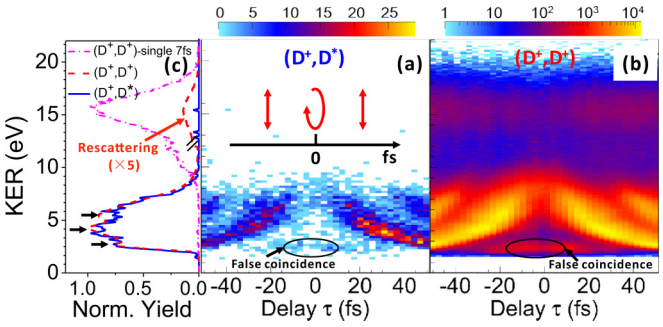

FIG. 2. The measured time-dependent nuclear KER spectra of the (a) (D^+, D^*) channel (linear scale) and (b) (D^+, D^+) channel (log scale) driven by few-cycle pump and probe pulses. (c) The normalized KER distributions of the (D^+, D^*) (blue solid curve), the (D^+, D^+) (red dashed curve) channels by integrating over all the time delay (the spectrum at KER >10 eV are scaled up by a factor of 5 to make it visible), and the (D^+, D^+) channel driven by a single linearly polarized 7-fs laser pulse (pink dot-dashed curve).

after the field ionization and acceleration by the electric field $E_i(\sim 1500\,\mathrm{V/cm})$ applied between the mesh and the MCP, which arrives at the detector earlier and was recorded as $(D^+, D^*)_{II}$ in the PIPICO spectrum.

As illustrated in Fig. 1(c), driven by few-cycle laser pulses in a pump-probe scheme, the dissociative FDI of D_2 can be understood as a sequential process, i.e., $D_2 \overset{\text{pump}}{\rightarrow} D_2{}^+ + e_1 \overset{\text{probe}}{\rightarrow} D^+ + D^+ + e_2 \Rightarrow D^+ + D^* + e$. By releasing the first electron e_1 from D_2 by the pump pulse, a NWP is launched onto the $1s\sigma_g$ state of $D_2{}^+$. The ionization-created NWP propagates outwards and may undergo up-and-down transitions between the $1s\sigma_g$ and $2p\sigma_u$ states ensured by the field-induced coupling. As the stretching molecular ion passing through the critical range of internuclear distance R, the second electron e_2 can tunnel out via CREI [16–19] induced by the subsequent probe pulse, leaving behind two bare deuterons which repel each other. In terms of the FTI picture [21], there is a certain probability that one of the freed electrons with a small drift momentum will be trapped by the combined effect of the ionic Coulomb potential and the oscillating laser field and eventually be captured by one of the ejected ionic D^+, resulting in the formation of excited neutral D^* populated on the high-lying Rydberg states.

The stepwise dynamics of dissociative FDI of D_2 can be revealed by tracing the kinetic-energy-release (KER) spectrum of the ejected nuclei as a function of the pump-probe time delay. The time-dependent KER spectra measured for the (D^+, D^*) and (D^+, D^+) channel with linearly and elliptically polarized few-cycle pump and probe pulses are displayed in Figs. 2(a) and 2(b), respectively. The negative and positive time delay correspond to the change of order in which the pulses of different polarizations arrived earlier, as illustrated in Fig. 1(a). The time-independent signals in the low-energy region close to zero time delay [indicated by the ellipses in Figs. 2(a) and 2(b)] are the false coincidence events that the measured nuclear fragments ejected from two individual molecules in the interaction region. The time-independent band structure around 16 eV of the (D^+, D^+) channel in Fig. 2(b) has been observed in previous studies (see, e.g., [12,44–46]) and originates from the electron rescattering induced nonsequential double ionization of D_2 molecules. The nonsequential double ionization occurs around the equilibrium internuclear distance of D_2 which is the main route for the (D^+, D^+) channel driven by a single linearly polarized 7-fs laser pulse, resulting in a similar KER around 16 eV as displayed in Fig. 2(c) (pink dot-dashed curve). The slightly reduced high-KER events around 16 eV at zero time delay is due to the deflection of the rescattering electron by the elliptically polarized pulse when it is temporally overlapped with the linearly polarized pulse. Since the bond stretching of the $D_2{}^+$ is demanded for the dissociative FDI, as shown in Figs. 2(a) and 2(c), the high-KER signal around 16 eV is absent in the (D^+, D^*) channel which excludes the noticeable contribution of the nonsequential double ionization process.

In contrast to the remarkable difference in the high-KER region around 16 eV, the time-dependent KER spectrum of the (D^+, D^*) channel is similar to that of the (D^+, D^+) channel in the low-KER region (KER <10 eV). The appeared periodical stripes with an interval of ~30 fs in the time-dependent KER spectra correspond to the vibrational oscillation of the NWPs in the bound state of the molecular ions. As the NWPs approach the outer turning point of the bound state, a portion of the NWPs would dissociate to the continuum or afterwards be field excited to produce the (D^+, D^*) or (D^+, D^+) channels by the time-delayed probe pulse. As shown in Fig. 2(c), since the high-lying Rydberg states are very close to the Coulombic repulsive curve of $1/R$, the time-integrated KER spectrum of the (D^+, D^*) channel in the low-KER region is very similar to that of the (D^+, D^+) channel. It is consistent with the scenario that the dissociative FDI channel proceeds in a similar approach as the dissociative sequential double ionization channel where two electrons are removed stepwise separated by the bond stretching. Moreover, as shown in Fig. 2(a), the yield of the (D^+, D^*) channels nearly vanishes at the zero time delay, but becomes visible when τ is larger (smaller) than 7 fs (−7 fs) for the positive (negative) time delay. It clearly indicates that the formation of the (D^+, D^*) pairs demands a time interval after the first ionization to ensure sufficient bond stretching of the molecular ion. This is consistent with the absence of the (D^+, D^*) channel driven by a single 7-fs laser pulse.

According to the intuitive picture of the FTI, the electron recapture probability is reduced with an increase of the laser ellipticity which deflects the motion of the tunneled electron [21]. Alternatively, the Rydberg state of atoms [47] and molecules [48] might be populated via the multiphoton excitation process which does not critically depend on the light polarization. In our experiments, we cannot exclude the contribution of the multiphoton excitation process in producing the (D^+, D^*) channel. Actually, the relatively increased (D^+, D^*) yield at positive time delay as compared to the negative time delay [Fig. 2(a)] might be ascribed to the multiphoton excitation in producing the (D^+, D^*) channel at a large internuclear distance of the stretched molecular ion by the latterly arrived elliptically polarized pulse whose intensity is higher than the linearly polarized pulse.

We will now address the essential question of which one of the two electrons released in the first and the second ionization steps will be eventually recaptured by the ionic core to form the (D^+, D^*) pair after the conclusion of the laser

fields. In a single multicycle laser pulse, both the first and the second ionization steps occur within the pulse duration and their individual contribution is hard to be distinguished. We overcome this difficulty by examining the laser-polarization-dependent momentum distributions of the detected electrons [49]. As sketched in Fig. 1(a), for the electron freed by a linearly polarized pulse, its final momentum will concentrate along the polarization direction (along the z axis in our experiment). However, for the elliptically polarized pulse, the electron is mainly freed when the laser field points along the major axis (along the z axis in our experiment) and ends up with a final momentum along the minor axis (along the y axis in our experiment) according to the angular streaking of the rotating laser field [18,50,51]. The distinct momentum distributions of the detected electrons allow us to identify whether they are from the first ionization step driven by the pump pulse or the second ionization step driven by the probe pulse.

Figure 3(a) displays the time-delay integrated momentum distribution of the freed electron measured in coincidence with the (D^+, D^*) pair. The electron released by the linearly polarized pulse is mainly concentrated within the yellow dashed ellipse along the z axis (denoted as e_{linear}), while the electron in the red dashed sectors along the y axis (denoted as $e_{\text{elliptical}}$) is released by the elliptically polarized pulse. For the dissociative FDI of D_2, since the two electrons are individually released by the few-cycle pump and probe pulses, the detection of the electron released by the pump pulse indicates the recapture of the electron released by the probe pulse, and vice versa.

The laser-polarization-dependent momentum distribution of the freed electron conspicuously encodes in the momentum vector along the y direction, i.e., $py_{e(\text{freed})}$. Figure 3(b) shows the distribution of $py_{e(\text{freed})}$ as a function of the time delay between the pump and probe pulses. For positive (negative) time delay, the linearly (elliptically) polarized pulse precedes the elliptically (linearly) polarized pulse. The $py_{e(\text{freed})}$ distribution at the positive time delay is noticeably different from that at the negative time delay. To make the features more intuitive, we plotted the one-dimensional distribution of $py_{e(\text{freed})}$ in Fig. 3(c) by integrating over the corresponding time delay. The three-peak structure of the $py_{e(\text{freed})}$ indicates that the detected freed electrons are released by laser pulse with different polarizations, namely the central peak around $py_{e(\text{freed})} = 0$ a.u. and the shoulders around $py_{e(\text{freed})} = +/-0.8$ a.u. are contributed by the linearly and elliptically polarized pulses, respectively.

We numerically fitted the $py_{e(\text{freed})}$ by assuming a multi-Gaussian distribution of the electron momentum centered at the central peak ($py_{e(\text{freed})} = 0$ a.u.) and at the two shoulders ($py_{e(\text{freed})} = +/-0.8$ a.u.) and shared a common width ω, as plotted by the solid curves in Fig. 3(c). For the multi-Gaussian distribution: $A_1 \times \exp[-0.5py_e{}^2/\omega^2] + A_2 \times \{\exp[-0.5(py_e + 0.8)^2/\omega^2] + \exp[-0.5(py_e - 0.8)^2/\omega^2]\}$, the amplitudes of A_1 and A_2 stand for the probabilities of the electron at the central peak and at the two shoulders, respectively. The distribution of $py_{e(\text{freed})}$ for the positive delay mostly concentrates along the center peak and the ratio of A_1/A_2 is estimated to be $\sim$1.86, while for the negative delay the distribution of the two shoulders is comparable to

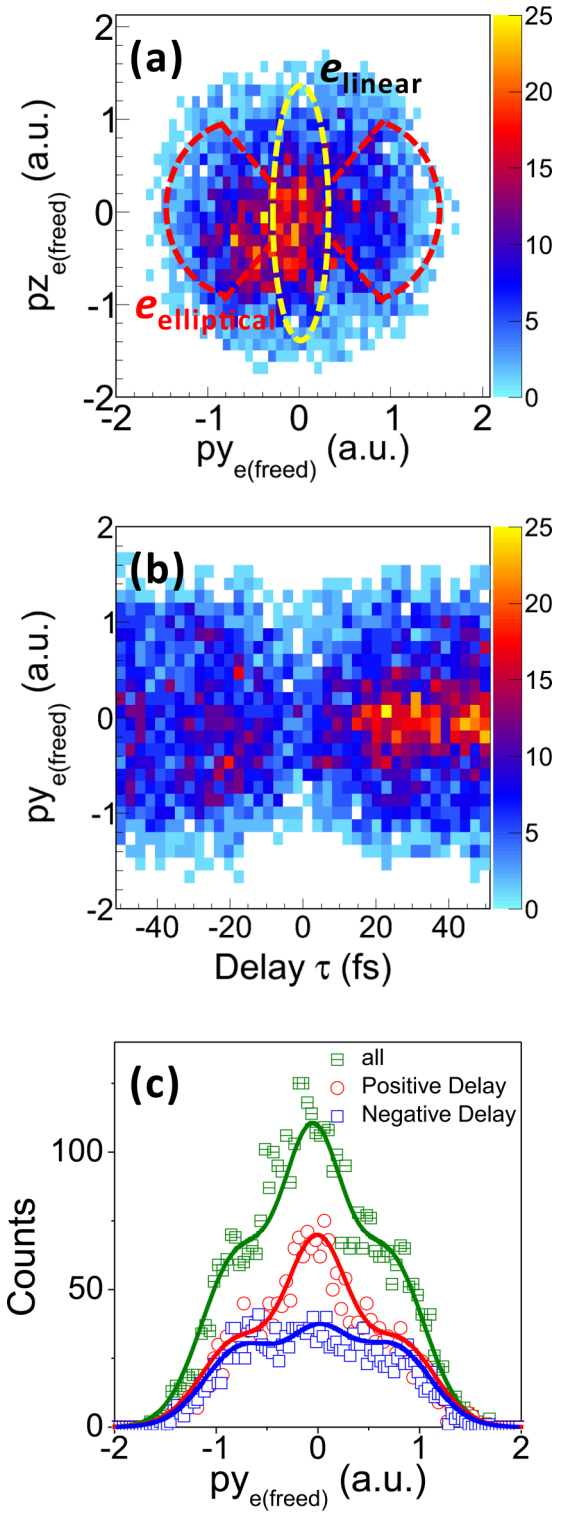

FIG. 3. (a) The momentum distributions of the detected photoelectron of the (D^+, D^*) channel integrated over the pump-probe time delay. Electrons distributed in the yellow dashed ellipse (e_{linear}) and the red dashed sectors ($e_{\text{elliptical}}$) are released by the linearly and elliptically polarized few-cycle pulses, respectively. (b) The time-dependent momentum distributions of the freed electron along the y axis. (c) The momentum distributions of $py_{e(\text{freed})}$ integrated over different time delay.

that of the center peak and the ratio of A_1/A_2 is estimated to be ∼1.1. The center peak of the observed three-peak structure of the $py_{e(\text{freed})}$ mainly results from the ionization induced by the linearly polarized pulse, while the two shoulders are mostly contributed by the ionization induced by the elliptically polarized pulse. For the positive delay, the linearly polarized pulse serves as the pump pulse to release the first electron and the elliptically polarized pulse as the probe to trigger the second ionization step. Likewise, for the negative delay, the pump pulse with elliptical polarization releases the first electron and the second electron is removed by the linearly polarized probe pulse. Thus, the characteristic of $py_{e(\text{freed})}$ distributions in the positive and negative time delay consistently imply that the detected freed electron is the first electron ionized by the pump pulse and the second electron released by the time delayed probe pulse is more likely to be recaptured to produce the (D^+, D^*) channel.

There are two routes for the dissociative FDI of molecules depending on whether the recaptured electron is released in the first or the second ionization steps [27]. The recapture of the electron released in the first ionization step strongly depends on the correlation between two released electrons; while the recapture of the electron released in the second ionization step prevails at a large internuclear distance where the CREI or multiphoton excitation occur. By using the few-cycle pump-probe scheme, the dissociative FDI channel was tracked to proceed in a sequential process where the two electrons of the molecule are released stepwise separated by the stretching of the molecular ion. In this sequential process, the correlation between the two released electrons is minor; while the CREI or multiphoton excitation of the stretched molecular ion is favorable around the critical internuclear distance. Our results show that the electron released in the second ionization step after the stretching of molecular ion is favored to be recaptured in the dissociative FDI of molecules.

IV. CONCLUSION

In conclusion, by utilizing linearly and elliptically polarized few-cycle laser pulses in a pump-probe scheme, we experimentally tracked the stepwise dynamics of the dissociative FDI of D_2 by monitoring the KER spectrum of the nuclear fragments and the momentum distribution of the freed electron as a function of the time delay. The ionic D^+, the excited neutral D^*, as well as the freed electron created from the dissociative FDI of D_2 were fully measured in coincidence in our reaction microscope. The detected electrons released by the pump or the probe pulses of different polarizations are distinguished by their momentum distributions. It enables us to deduce the recapture of the electron released from the first or the second ionization steps. Although the electron released from both ionization steps can be recaptured [27], our results show that the electron released in the second ionization step is preferred to be recaptured by the ionic core in producing the dissociative FDI channel of molecules in strong laser fields.

ACKNOWLEDGMENTS

We thank F. He for the fruitful discussions. This work was supported by the National Key R&D Program of China (Grant No. 2018YFA0306303), the National Natural Science Fund (Grants No. 11425416, No. 61690224, No. 11761141004, and No. 11704124), the 111 project of China (Grant No. B12024), and the Shanghai Sailing Program (Grant No. 17YF1404000).

[1] P. H. Bucksbaum, A. Zavriyev, H. G. Muller, and D. W. Schumacher, Phys. Rev. Lett. **64**, 1883 (1990).
[2] G. Yao and S.-I Chu, Phys. Rev. A **48**, 485 (1993).
[3] L. J. Frasinski, J. H. Posthumus, J. Plumridge, K. Codling, P. F. Taday, and A. J. Langley, Phys. Rev. Lett. **83**, 3625 (1999).
[4] M. Magrakvelidze, F. He, T. Niederhausen, I. V. Litvinyuk, and U. Thumm, Phys. Rev. A **79**, 033410 (2009).
[5] K. Liu, P. Lan, C. Huang, Q. Zhang, and P. Lu, Phys. Rev. A **89**, 053423 (2014).
[6] W. Zhang, Z. Li, P. Lu, X. Gong, Q. Song, Q. Ji, K. Lin, J. Ma, F. He, H. Zeng, and J. Wu, Phys. Rev. Lett. **117**, 103002 (2016).
[7] L. Yue and L. B. Madsen, Phys. Rev. A **93**, 031401 (2016).
[8] W. Zhang, H. Li, K. Lin, P. Lu, X. Gong, Q. Song, Q. Ji, J. Ma, H. X. Li, H. Zeng, F. He, and J. Wu, Phys. Rev. A **96**, 033405 (2017).
[9] P. Lu, J. Wang, H. Li, K. Lin, X. Gong, Q. Song, Q. Ji, W. Zhang, J. Ma, H. X. Li, H. Zeng, F. He, and J. Wu, Proc. Natl. Acad. Sci. USA **115**, 2049 (2018).
[10] H. Niikura, F. Légaré, R. Hasbani, A. D. Bandrauk, M. Yu. Ivanov, D. M. Villeneuve, and P. B. Corkum, Nature (London) **417**, 917 (2002).
[11] H. Sakai, J. J. Larsen, I. Wendt-Larsen, J. Olesen, P. B. Corkum, and H. Stapelfeldt, Phys. Rev. A **67**, 063404 (2003).
[12] A. S. Alnaser, T. Osipov, E. P. Benis, A. Wech, B. Shan, C. L. Cocke, X. M. Tong, and C. D. Lin, Phys. Rev. Lett. **91**, 163002 (2003).
[13] H. Stapelfeldt, E. Constant, and P. B. Corkum, Phys. Rev. Lett. **74**, 3780 (1995).
[14] B. D. Esry, A. M. Sayler, P. Q. Wang, K. D. Carnes, and I. Ben-Itzhak, Phys. Rev. Lett. **97**, 013003 (2006).
[15] A. Hishikawa, A. Iwamae, K. Hoshina, M. Kono, and K. Yamanouchi, Chem. Phys. **231**, 315 (1998).
[16] T. Zuo and A. D. Bandrauk, Phys. Rev. A **52**, R2511 (1995).
[17] S. Chelkowski, A. D. Bandrauk, A. Staudte, and P. B. Corkum, Phys. Rev. A **76**, 013405 (2007).
[18] J. Wu, M. Meckel, L. Ph. H. Schmidt, M. Kunitski, S. Voss, H. Sann, H. Kim, T. Jahnke, A. Czasch, and R. Dörner, Nat. Commun. **3**, 1113 (2012).
[19] X. Gong, Q. Song, Q. Ji, H. Pan, J. Ding, J. Wu, and H. Zeng, Phys. Rev. Lett. **112**, 243001 (2014).
[20] B. B. Wang, X. F. Li, P. M. Fu, J. Chen, and J. Liu, Chin. Phys. Lett. **23**, 2729 (2006).
[21] T. Nubbemeyer, K. Gorling, A. Saenz, U. Eichmann, and W. Sandner, Phys. Rev. Lett. **101**, 233001 (2008).
[22] U. Eichmann, T. Nubbemeyer, H. Rottke, and W. Sandner, Nature (London) **461**, 1261 (2009).
[23] S. Eilzer and U. Eichmann, J. Phys. B **47**, 204014 (2014).

[24] S. Larimian, C. Lemell, V. Stummer, J. W. Geng, S. Roither, D. Kartashov, L. Zhang, M. X. Wang, Q. Gong, L. Y. Peng, S. Yoshida, J. Burgdörfer, A. Baltuška, M. Kitzler, and X. Xie, Phys. Rev. A **96**, 021403(R) (2017).
[25] B. Manschwetus, T. Nubbemeyer, K. Gorling, G. Steinmeyer, U. Eichmann, H. Rottke, and W. Sandner, Phys. Rev. Lett. **102**, 113002 (2009).
[26] K. N. Shomsky, Z. S. Smith, and S. L. Haan, Phys. Rev. A **79**, 061402(R) (2009).
[27] A. Emmanouilidou, C. Lazarou, A. Staudte, and U. Eichmann, Phys. Rev. A **85**, 011402(R) (2012).
[28] T. Nubbemeyer, U. Eichmann, and W. Sandner, J. Phys. B **42**, 134010 (2009).
[29] J. McKenna, S. Zeng, J. J. Hua, A. M. Sayler, M. Zohrabi, N. G. Johnson, B. Gaire, K. D. Carnes, B. D. Esry, and I. Ben-Itzhak, Phys. Rev. A **84**, 043425 (2011).
[30] B. Ulrich, A. Vredenborg, A. Malakzadeh, M. Meckel, K. Cole, M. Smolarski, Z. Chang, T. Jahnke, and R. Dörner, Phys. Rev. A **82**, 013412 (2010).
[31] B. Manschwetus, H. Rottke, G. Steinmeyer, L. Foucar, A. Czasch, H. Schmidt-Böcking, and W. Sandner, Phys. Rev. A **82**, 013413 (2010).
[32] J. Wu, A. Vredenborg, B. Ulrich, L. Ph. H. Schmidt, M. Meckel, S. Voss, H. Sann, H. Kim, T. Jahnke, and R. Dorner, Phys. Rev. Lett. **107**, 043003 (2011).
[33] X. Xie, C. Wu, H. Liu, M. Li, Y. Deng, Y. Liu, Q. Gong, and C. Wu, Phys. Rev. A **88**, 065401 (2013).
[34] W. Zhang, Z. Yu, X. Gong, J. Wang, P. Lu, H. Li, Q. Song, Q. Ji, K. Lin, J. Ma, H. X. Li, F. Sun, J. Qiang, H. Zeng, F. He, and J. Wu, Phys. Rev. Lett. **119**, 253202 (2017).
[35] R. Dörner, V. Mergel, O. Jagutzki, L. Spielberger, J. Ullrich, R. Moshammer, and H. Schmidt-Böcking, Phys. Rep. **330**, 95 (2000).
[36] J. Ullrich, R. Moshammer, A. Dorn, R. Dörner, L. P. H. Schmidt, and H. Schmidt-Böcking, Rep. Prog. Phys. **66**, 1463 (2003).
[37] Ben Berry, M. Zohrabi, D. Hayes, U. Ablikim, Bethany Jochim, T. Severt, K. D. Carnes, and I. Ben-Itzhak, Rev. Sci. Instrum. **86**, 046103 (2015).
[38] T. F. Gallagher, *Rydberg Atoms* (Cambridge University Press, Cambridge, England, 2005), Vol. 6.
[39] H. Zimmermann, J. Buller, S. Eilzer, and U. Eichmann, Phys. Rev. Lett. **114**, 123003 (2015).
[40] E. Diesen, U. Saalmann, M. Richter, M. Kunitski, R. Dörner, and J. M. Rost, Phys. Rev. Lett. **116**, 143006 (2016).
[41] H. Lv, W. Zuo, L. Zhao, H. Xu, M. Jin, D. Ding, S. Hu, and J. Chen, Phys. Rev. A **93**, 033415 (2016).
[42] S. Larimian, S. Erattupuzha, C. Lemell, S. Yoshida, S. Nagele, R. Maurer, A. Baltuška, J. Burgdörfer, M. Kitzler, and X. Xie, Phys. Rev. A **94**, 033401 (2016).
[43] M. J. Rakovic and S.-I. Chu, J. Phys. B **31**, 1989 (1998).
[44] A. Staudte, C. L. Cocke, M. H. Prior, A. Belkacem, C. Ray, H. W. Chong, T. E. Glover, R. W. Schoenlein, and U. Saalmann, Phys. Rev. A **65**, 020703(R) (2002).
[45] A. S. Alnaser, X. M. Tong, T. Osipov, S. Voss, C. M. Maharjan, P. Ranitovic, B. Ulrich, B. Shan, Z. Chang, C. D. Lin, and C. L. Cocke, Phys. Rev. Lett. **93**, 183202 (2004).
[46] F. Légaré, I.V. Litvinyuk, P.W. Dooley, F. Quéré, A. D. Bandrauk, D. M. Villeneuve, and P. B. Corkum, Phys. Rev. Lett. **91**, 093002 (2003).
[47] Q. Li, X.-M. Tong, T. Morishita, H. Wei, and C. D. Lin, Phys. Rev. A **89**, 023421 (2014).
[48] H. Lv, J. Zhang, W. Zuo, H. Xu, M. Jin, and D. Ding, Chin. Phys. B **24**, 063303 (2015).
[49] Q. Song, Z. Li, S. Cui, P. Lu, X. Gong, Q. Ji, K. Lin, W. Zhang, J. Ma, H. Pan, J. Ding, M. F. Kling, H. Zeng, F. He, and J. Wu, Phys. Rev. A **94**, 053419 (2016).
[50] P. Eckle, A. N. Pfeiffer, C. Cirelli, A. Staudte, R. Dörner, H. G. Muller, M. Büttiker, and U. Keller, Science **322**, 1525 (2008).
[51] A. N. Pfeiffer, C. Cirelli, M. Smolarski, R. Dörner, and U. Keller, Nat. Phys. **7**, 428 (2011).